Selective Ion Pairing in [Ir(bipy)$H_2(PRPh_2)_2$]A (A = PF_6, BF_4, CF_3SO_3, BPh_4, R = Me, Ph): Experimental Identification and Theoretical Understanding

Alceo Macchioni,*,† Cristiano Zuccaccia,† Eric Clot,*,‡ Karin Gruet,§ and Robert H. Crabtree*,§

Dipartimento di Chimica, Università di Perugia, Via Elce di Sotto 8, 06123 Perugia, Italy, L.S.D.S.M.S. (UMR 5636), Case Courrier 14, Université de Montpellier II, 34095 Montpellier Cedex 5, France, and Department of Chemistry, Yale University, 225 Prospect Street, New Haven, Connecticut 06520-8107

Received January 4, 2001

NMR studies of the title compounds show that selective tight ion pairing occurs with the anion binding site being located in an intuitively unexpected region of the cation: on the side of the bipyridyl ligand remote from the metal instead of being closest to the metal near the MH_2 group. The interaction specificity falls off with increasing anion size. ONIOM (QM/MM) calculations represent the cation structure very well, and natural population analysis calculations identify the predominant location of the positive charge at the bipyridyl ring carbons that take part in the inter-ring C−C bond (C-2 and C-2′). This is fully consistent with tight ion pairing near these and the adjacent carbons, C-3 and C-3′. The electrostatic potential calculated for the cation confirms the location of the preferred binding site.

Introduction

Even though ion pairing is recognized in coordination and organometallic compounds and is known to influence reaction rate,[1,2] it is often ignored in the majority of discussions of organometallic structure and mechanism. Metallocene polymerization is one area where ion pairing both has a clearly important mechanistic role and has been carefully studied.[3] The structure of ion pairs has sometimes been inferred from X-ray structural work, where it is assumed that the solution structure, the only structure relevant to reactivity in solution, is the same as in the solid.

An early finding of the possible influence of the counteranion on the stability of compounds was made by Bianchini et al.[4] Depending on the counteranion used, they obtained in the solid state either a dihydrogen cobalt complex with BPh_4 or a dihydride cobalt complex with PF_6, whereas in solution only the dihydrogen isomer is seen for both counteranions.

Morris and co-workers detected a "bifurcated" hydrogen bonding involving a hydride, a proton from a pendant neighboring amino group, and a fluorine of the counteranion BF_4, Ir−H···H(N)···F−B.[5] Indeed, a previous attempt to disrupt the expected Ir−H···H−N hydrogen bond with the use of another acceptor, $OPPh_3$, failed. The crystallographic structural analysis showed that the hydrogen on the nitrogen and a fluorine of the counteranion are close, in the range of possible hydrogen bonding. In other work,[6] one of the fluorines of the counteranion BF_4 is found to hydrogen bond to a proton of two different NH groups, which are themselves hydrogen bonded to a hydride, making a hydrogen-bonded four-membered ring. This interaction is seen in the X-ray structure analysis as well as in the low-temperature ^{1}H NMR, but is not seen in the low-temperature ^{19}F NMR.

Macchioni, Ruegger, Venanzi, and their co-workers have applied ^{1}H NOESY and ^{19}F{^{1}H} HOESY NMR spectroscopy to the investigation of predominant ion pair solution structures of organometallic complexes by the detection of interionic contacts.[7,8] The results suggest that these ion pairs have surprisingly well-defined structures, often broadly similar to the solid-state structure. For example, in one case, the anion is surrounded in the solid state by six symmetry-related cations, only one of which reflects the solution structure.[9b] In such a case, even with the solid-state structure in hand, it would not be obvious which of the ion pairs seen in the solid would resemble the solution structure. One

* Corresponding authors. E-mail: alceo@unipg.it, clot@lsd.univ-montp2.fr, robert.crabtree@yale.edu.
† Università di Perugia.
‡ Université de Montpellier II.
§ Yale University.

(1) Romeo, R.; Arena, G.; Scolaro, L. M.; Plutino, M. R. *Inorg. Chim. Acta* **1995**, *241*, 81.
(2) Bellachioma, G.; Cardaci, G.; Macchioni, A.; Zuccaccia, C. *J. Organomet. Chem.* **2000**, *594*, 119.
(3) Chen, Y. X.; Metz, M. V.; Li, L. T.; Stern, C. L.; Marks, T. J. *J. Am. Chem. Soc.* **1998**, *120*, 6287.
(4) Bianchini, C.; Mealli, C.; Peruzzini, M.; Zanobini, F. *J. Am. Chem. Soc.* **1992**, *114*, 5905.
(5) Park, S.; Lough, A. J.; Morris, R. H. *Inorg. Chem.* **1996**, *35*, 3001.
(6) Xu, W.; Lough, A. J.; Morris, R. H. *Inorg. Chem.* **1996**, *35*, 1549.
(7) Bellachioma, G.; Cardaci, G.; Macchioni, A.; Reichenbach, G.; Terenzi, S. *Organometallics* **1996**, *15*, 4349.
(8) Macchioni, A.; Bellachioma, G.; Cardaci, G.; Gramlich, V.; Rüegger, H.; Terenzi, S.; Venanzi, L. M. *Organometallics* **1997**, *16*, 2139.
(9) (a) Macchioni, A.; Bellachioma, G.; Cardaci, G.; Travaglia, M.; Zuccaccia, C.; Milani, B.; Corso, G.; Zangrando, E.; Mestroni, G.; Carfagna, C.; Formica, M. *Organometallics* **1999**, *18*, 3061. (b) Macchioni, A.; Bellachioma, G.; Cardaci, G.; Cruciani, G.; Foresti, E.; Sabatino, P.; Zuccaccia, C. *Organometallics* **1998**, *17*, 5549.

10.1021/om010015l CCC: $20.00
Publication on Web 05/01/2001

trend evident from prior work[7,8,9b,10] is that the anion tends to prefer to remain in the vicinity of any N-heterocyclic ligand, such as a pyridyl or pyrazolyl group. It was not clear if this would continue to be true if the complex had a cis-MH_2 group present. Such a sterically small group, also potentially able to hydrogen bond to the anion, might attract the counterion because in this way it could approach much more closely to the central metal. Prior work had not used computational methods to characterize the PE surface around the cation and predict the ion pair structure.

In our work on Ir hydrides, we have seen anion effects that made us consider ion pairing as an issue. One goal of this paper was to find the solution ion pair structure for $[IrH_2(bipy)(PRPh_2)_2]A$ (**1**,**2**, bipy = 2,2′-bipyridyl; R = Ph, A = BF_4, PF_6, CF_3SO_3, and BPh_4; R = Me, A = PF_6) and compare it with the solid-state structures (**1b**,**c**). As the smallest ligand, a hydride might be thought to favor ion pairing in its vicinity so that the metal···anion distance would be minimized. Cationic metal hydrides can be weakly acidic and can even hydrogen bond, as in M−H···base interactions,[11] so the ion pairing might no longer take place as in prior cases near the bipy ligand. We find that both **1b** and **1c** have dissimilar solid and solution structures, but in both cases the anion prefers the vicinity of the bipyridyl ligand to the vicinity of the hydrides, where it could approach much closer to the central metal. Consistent with experiment, theoretical work locates the positive charge on the inter-ring carbons, C-2 and C-2′, of the bipy ligand and not on the metal or bipy nitrogens as previously assumed.

Results and Discussion

Synthesis of Compounds 1a−d and 2. Pignolet et al.[12,13] and Crabtree et al.[14] previously reported the syntheses of complexes **1a**−**c**. **1a** was obtained by the reaction of the bis-solvento complex $[Ir(PPh_3)_2(acetone)_2(H)_2]BF_4$ and 2,2′-bipyridyl, and **1b** by metathesis of **1a** with NH_4PF_6.[12,13] Here, we report a modified procedure for the preparation of complexes **1** and **2**. A methylene chloride solution of $[Ir(cod)(PRPh_2)_2]X$ and 2,2′-bipyridyl was treated with dihydrogen gas at 0 °C to give *cis*,*trans*-$[IrH_2(bipy)(PRPh_2)_2]X$ (**1**, **2**) in good yields. Complexes **1** and **2** were fully characterized by elemental analysis and IR, ^1H, ^{13}C, ^{31}P, and ^{19}F NMR spectroscopies. The spectroscopic data of **1a**−**c** are consistent with those in the literature.[12−14] The data for the new complexes **1d** and **2**, presented below, are closely similar to those of **1a**−**c**.

NMR Intramolecular Characterization. The structure of complexes **1** and **2**, shown in Chart 1, was investigated in methylene chloride-d_2 by ^1H, ^{13}C, ^{31}P, and ^{19}F NMR spectroscopies. The assignments of all the ^1H and ^{13}C resonances were performed following the scalar and dipolar nuclear interactions in the ^1H COSY, ^1H, ^{13}C HMQC, and ^1H NOESY experiments, respectively. The assignment of the protons of the bipy rings was carried out starting from the observation of an NOE contact between proton H-6 and hydride H-1″ (Figure 1). The ^1H NMR spectrum of compound **2** displays a triplet resonance at −19.87 ppm ($^2J_{HP}$ = 16.8 Hz) for the two equivalent hydrides H-1″ and H-2″, a signal at 1.88 ppm for the methyl protons, and a complex multiplet ranging from 7.08 to 8.46 ppm for the phenyl and bipyridyl protons. All numbering refers to Chart 1.

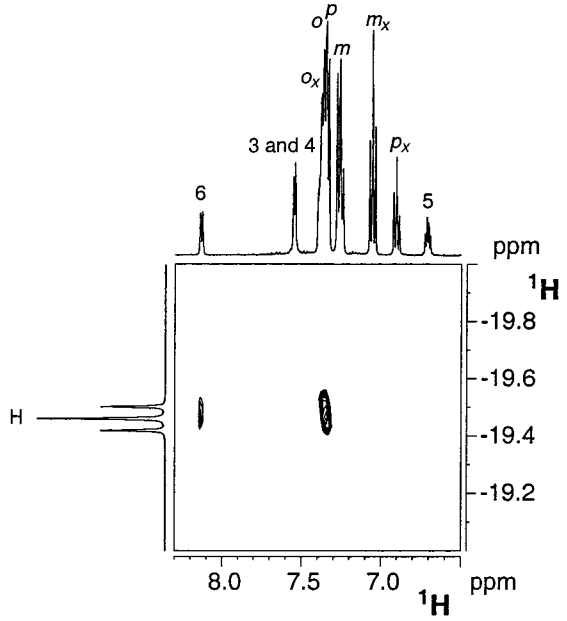

Figure 1. Section of the ^1H−NOESY NMR spectrum of complex **1d** recorded at 400.13 MHz in methylene chloride-d_2 (298 K) showing the selective intramolecular interactions of the hydrides with protons H-6 and H-*o*.

Chart 1

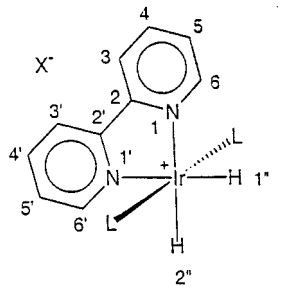

L = PPh_3 X = BF_4 (**1a**)
X = PF_6 (**1b**)
X = CF_3SO_3 (**1c**)
X = BPh_4 (**1d**)
L = $PMePh_2$ X = PF_6 (**2**)

NMR Interionic Investigations. The relative anion−cation position (interionic structure)[10] of complexes **1** and **2** was investigated in methylene chloride-d_2 by dissolving about 20 mg of compound in 0.6 mL of solvent. Under these conditions, the complexes are mainly present in solution as intimate ion pairs,[15] and dipolar interactions between nuclei belonging to the two ionic moieties can be detected in the ^1H NOESY or ^{19}F-{^1H} HOESY spectra. As shown in Figure 2, the nuclei

(10) Zuccaccia, C.; Bellachioma, G.; Cardaci, G.; Macchioni, A. *Organometallics* **1999**, *18*, 1, and references therein.
(11) Desmurs, P.; Kavallieratos, K.; Yao, W.; Crabtree, R. H. *New J. Chem.* **1999**, *23*, 1111.
(12) Alexander, B. D.; Johnson, B. J.; Johnson, S. M.; Casalnuevo, A. L.; Pignolet, L. H. *J. Am. Chem. Soc.* **1986**, *108*, 4409.
(13) Alexander, B. D.; Johnson, B. J.; Johnson, S. M.; Boyle, P. D.; Kann, N. C.; Pignolet, L. H. *Inorg. Chem.* **1987**, *26*, 3506.
(14) Guzei, I. A.; Rheingold, A. L.; Lee, D.-H.; Crabtree, R. H. *Z. Kristallogr.−New Cryst. Struct.* **1998**, *213*, 585.

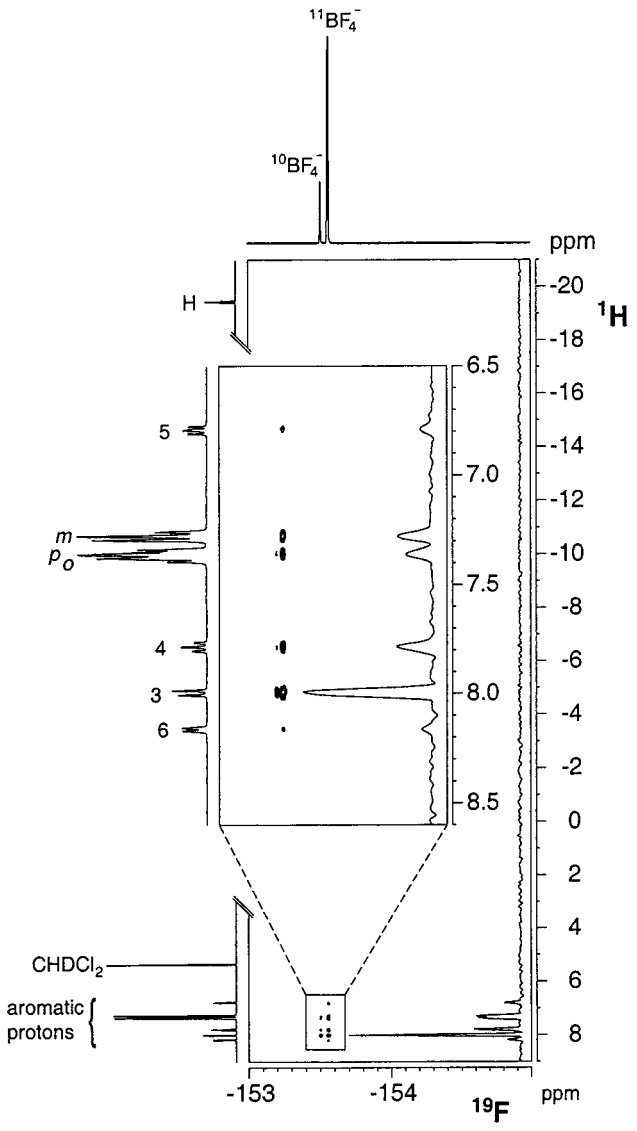

Figure 2. $^{19}F\{^1H\}$ HOESY NMR spectrum of complex **1a** recorded at 376.63 MHz in methylene chloride-d_2 (298 K) showing (a) the absence of the "expected" interionic NOE between the hydrides and the anion and (b) the contacts between BF_4^- and aromatic protons. In the expansion the point (b) is better illustrated and the interaction intensity order 3 > 4 > 5 > 6 is shown. The 1D-trace relative to the $^{11}BF_4^-$ column is reported on the right of both total spectrum and expansion.

of the counteranion of complexes **1** interact with protons H-3,3′ (strong), H-4,4′ (medium), H-5,5′ (weak), H-*m* (very weak), H-*o* (very weak), and H-6,6′ (very weak).[16] The intensities of the interionic NOE interactions are reported in Table 1, by arbitrarily fixing, in every complex, the highest value to 1 (X^- with proton 3). Even though the data of Table 1 have little absolute meaning, they can be useful to understand how the strength of X^-/aromatic proton interactions, relative to that of X^-/proton 3, is affected by the change of counteranion. No contact is observed with the two hydrides H-1″ and H-2″. This is true independent of the nature of the counterion. The interactions are practically the same in complex **2**, with the addition of a weak interaction between the phosphine Me protons and PF_6^-. The observed anion−cation "contacts" afford a well-defined structure for the ion pair: the anion is located close to protons H-3,3′, as reported in Chart 1. The expected localization of the counterion close to the hydride region, which should allow a minimal metal anion distance, is not observed. This suggests that the positive charge is not localized on iridium, but is predominantly delocalized onto the bipyridyl ligand, as already observed in previous studies, where the nitrogens were considered as the predominant positive centers.[9] In complex **1d**, protons close to the counteranion are shielded by the π-electrons[17a] of the BPh_4^- aromatic rings, as expected from the NOE-deduced interionic structure. For a quantitative comparison with the data from NOE measurements the $\Delta\delta_H$ (ppm) data, normalized with respect to protons H-3,3′, should be raised to the half power to take into account that the shielding effect is a first-order dipole−dipole interaction ($\propto 1/r^3$),[17a] while the NOE is a second-order relaxation effect ($\propto 1/r^6$). The $\Delta\delta_H$ (ppm) of the bipy protons for **1a**−**d** perfectly follows the trend of NOE results (Table 1) with the degree of interaction falling in the order 3 > 4 > 5 > 6. Furthermore, from Table 1 it can be concluded that the highest specificity of anion−cation interactions is reached with the smallest anion (BF_4^-). As an example, the intensity of the interaction between the counteranion and the H-4 proton relative to that with H-3 increases with increasing anion size: 0.33 (**1a**) < 0.38 (**1b**) < 0.57 (**1c**) < 0.71 (**1d**). The size of the counteranion plays a role in its location around the cation, as well as the strength of the interaction with the cation.

Table 1. Quantification of the Anion−Cation Interactions

	1a[a]	**1b**[a]	**1c**[a]	**1d**[b]
3	1.00	1.00	1.00	1.00
4	0.33	0.38	0.57	0.71
5	0.11	0.16	0.27	0.45
6	0.06	0.06	0.11	0.24

[a] Values derived from the integration of NOE "contacts" normalized with respect to protons H-3,3′. [b] Values derived from the shielding exerted by the π-electrons[17a] of BPh_4^- normalized with respect to the $\Delta\delta$(**1a**−**d**) value of protons H-3,3′. The $\Delta\delta$ values were raised to the 1/2 power in order to be quantitatively comparable with the data from NOE measurements.

X-ray Crystallographic Characterization of Complexes 1b and 1c. The structures of complexes [IrH$_2$(bipy)(PPh$_3$)$_2$]A **1b** (A = PF_6) and **1c** (A = CF_3SO_3) were previously reported (Figures 3 and 4).[13,14] In both compounds, the ligands around the central metal are found in an essentially octahedral arrangement, with the bipyridyl and the two hydride ligands in the plane of the molecule. Distances are normal. The outer sphere A^- anions are located close to the H-6 and H-5 positions, but far away from H-6′ and H-5′ positions of the

(15) Zuccaccia, C.; Bellachioma, G.; Cardaci, G.; Macchioni, A. *Organometallics* **2000**, *19*, 4663. Bellachioma, G.; Cardaci, G.; Macchioni, A.; Zuccaccia, C. Unpublished conductometric results relative to octahedral Ru(II) complexes.

(16) From the 1D-traces reported in Figure 2 it could appear that NOEs relative to the interionic interactions of *o* and *m* protons with BF_4^- have the same intensity as that of protons H-4,4′. In reality, it must be considered that for a quantitative comparison the NOE intensity has to be divided by the number of equivalent protons, i.e., 12 and 2 for *o*/*m* and bipy protons, respectively. The intensity of the interionic interaction of the *o* and *m* protons becomes similar to that of protons H-4,4′.

(17) (a) Haigh, C. W.; Mallion, R. B. *Prog. NMR Spectrosc.* **1980**, *13*, 303. (b) Harris, R. K. *Can. J. Chem.* **1964**, *42*, 2275.

Table 2. Selected Nonbonded Interionic Distances (Å) for Compound 1b and 1c[a]

1b		1c	
H1″−F6	3.068	H1″−F2	5.488
H2″−F6	5.002	H2″−F2	7.419
		H1″−O2	4.154
		H2″−O2	6.423
H6−F1	2.957	H6−O2	2.843
H5−F1	3.744	H5−O2	3.871
H4−F1	6.042	H4−O2	6.171
H3−F1	7.272	H3−O2	7.313
		H6−O3	3.215
		H5−O3	2.509
		H4−O3	4.744
		H3−O3	6.516
H6′−F1	8.709	H6′−O2	8.536

[a] Calculated from the crystal structures with H ligands in calculated positions. Numbers refer to Chart 1.

bipyridyl ligand, and close to the hydride H-1″, but far away from the hydride H-2″. Table 2 shows a selection of the shortest nonbonded interionic distances, which were obtained from the crystal structures of **1b** and **1c** registered in the Cambridge Structural Database System. The expected localization of the counteranion close to both hydrides is not observed; indeed the counteranion is located close to one hydride and to one side of the bipyridyl ligand. However, the counteranion PF_6^- is closer to the metal center than $CF_3SO_3^-$, which was expected since $CF_3SO_3^-$ is larger than PF_6^-; thence $CF_3SO_3^-$ cannot approach the metal center as easily due to steric interactions with nearby bipyridyl and phosphine ligands. This anion−cation specificity was also encountered in solution.

Solid-State vs Solution Interionic Structures of Complexes 1a and 1c. The analysis of the spectroscopic data obtained in solution leads to the conclusion that the counteranion is located close to protons H-3 and H-4 of the bipyridyl ligand, far away from the two hydrides, whereas in the solid state the counteranion is found close to one of the hydrides (H-1″) and close to protons H-6 and H-5 of the bipyridyl ligand.

To elucidate this difference, we carried out hybrid quantum mechanics (QM)/molecular mechanics (MM) calculations on the complex $Ir(H)_2(bipy)(PPh_3)_2^+$. Density functional theory (B3PW91) calculations were carried out on $Ir(H)_2(bipy)(PH_3)_2^+$ as a QM model, and phenyl substituents were treated at the MM level (UFF force field) within the ONIOM methodology (see Computational Details for further information).

The optimized geometry (ONIOM) of $Ir(H)_2(bipy)(PPh_3)_2^+$ is shown in Figure 5, and some geometrical parameters are given in Table 3 for comparison with the published X-ray data for $[Ir(H)_2(bipy)(PPh_3)_2][CF_3SO_3]$[14] and $[Ir(H)_2(bipy)(PPh_3)_2][PF_6]$.[13] The ONIOM geometry is in very good agreement with the experimental data, and the disymmetry between the two Ir−N bonds is particularly well reproduced. π-Stacking interactions are present between the pyridine and phenyl rings, and these stabilizing interactions are most likely responsible for the distortion. The simulation of such a subtle effect with ONIOM clearly illustrates the sensitivity and the strength of this hybrid QM/MM method.

We performed a natural population analysis (NPA) which shows that the positive charge is not localized on the IrH_2 part of the molecule. The NPA charges on the hydrides are −0.015 and −0.026, indicating a weak

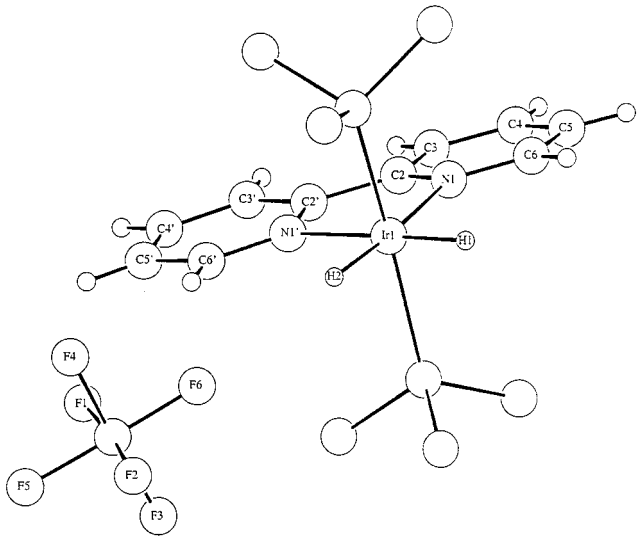

Figure 3. View of the solid-state structure of complex **1b** generated from CSDS. Crystallographic numbering applies.

hydridic character. Moreover the charge on iridium is also negative, with a value of −0.13. This negative charge is a combination of two effects. The phosphines (PH_3) are rather basic; thence some electron density is transferred to the Ir. As a result, the global charge on each PH_3 ligand is +0.42. The other contributing effect to the negative charge on Ir is π-donation from the nitrogen atoms; indeed the NPA occupation of the $2p_z$ orbital (perpendicular to the bipy plane) is only 1.28, indicating π-donation from nitrogen to iridium.

However, both nitrogen atoms are negatively charged (−0.55) as a consequence of the bonding interactions with neighboring positively charged carbon atoms C-2 (+0.21) and C-6 (+0.09). The other carbon atoms of the bipy ring are negatively charged: −0.24 for C-5, −0.16 for C-4, and −0.22 for C-3. The negative charge on nitrogen is mainly a consequence of σ-type interactions causing a drift of electron density from the adjacent atoms to nitrogen. The total NPA population of orbitals 2s, $2p_x$, and $2p_y$, from which the sp^2 hybrids are constructed, is 4.22, leading to a "σ-charge" of −1.22 compensated by a "π-charge" of +0.72 to give an overall charge of ca. −0.5. Although σ-type density originates from Ir, C-2, and C-6, the π-donation from nitrogen is essentially directed toward iridium.

This charge analysis clearly shows that the positive charge is located on the phosphine ligands and on the carbon atoms C-2 and C-2′ that form the inter-ring C−C bond of the bipy ligand. The use of PH_3 as a model phosphine is a limitation here, and the real phosphines, PPh_3, are certainly less positively charged. Even if the P atoms bear some positive charge, they will be buried in the bulk of the three phenyl rings and would not be involved in any strong interaction with the counteranion. However the presence of positive charge on carbons C-2 and C-2′ is in very good agreement with the NMR experiment and is clearly consistent with the location of the counteranion.

We also computed the electrostatic potential created by the molecule, and a contour plot in the plane of the bipy ligand is shown as Figure 6. As expected for a positively charged molecule, the electrostatic potential is positive, leading to global attraction for an anion.

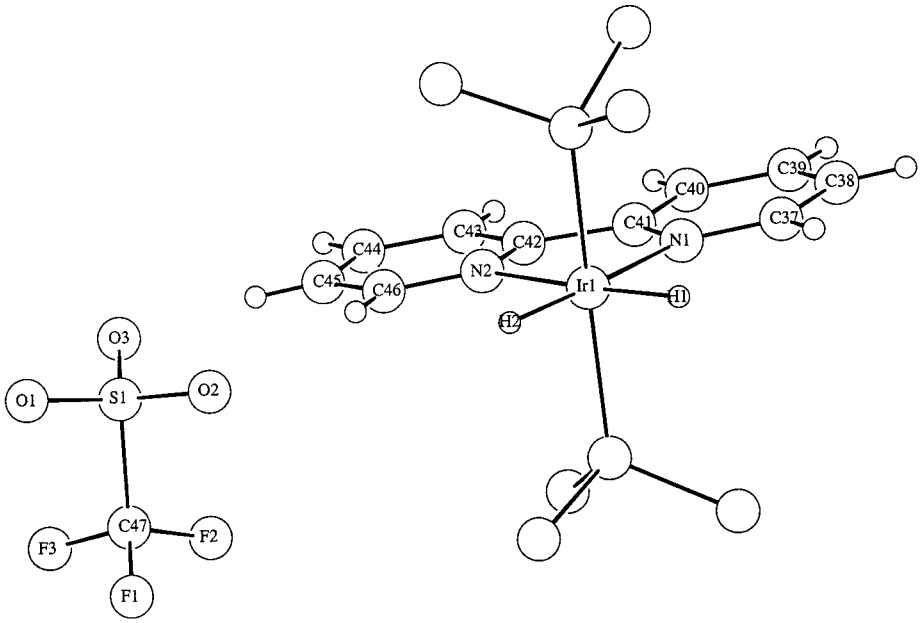

Figure 4. View of the solid-state structure of complex **1c** generated from CSDS. Crystallographic numbering applies.

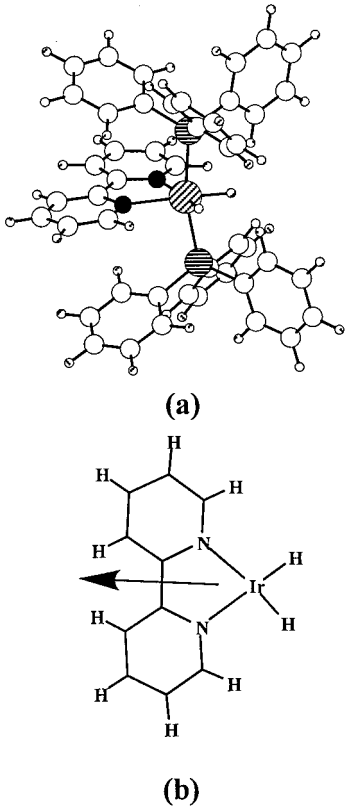

Figure 5. (a) Optimized geometry (ONIOM) for Ir(H)$_2$-(bipy)(PPh$_3$)$_2^+$. (b) Schematic representation of the QM part in the ONIOM calculations (PH$_3$ groups have been omitted for clarity) showing the orientation of the dipole moment of the molecule.

However, the topology of the potential is in favor of a preferred interaction in the vicinity of C-2 and C-2′. There is a smooth attractive valley pointing toward the midpoint of the C-2−C-2′ bond, in perfect agreement with the NMR experiment. Moreover the electrostatic potential clearly shows that the IrH$_2$ region is the less attractive region despite its lower steric bulk. This is in agreement with the charge analysis, which gave negative charges for IrH$_2$.

Table 3. Comparison between Selected Experimental[13,14] and Calculated Bond Distances (Å) and Angles (deg) for Ir(H)$_2$(bipy)(PPh$_3$)$_2^+$[a]

	ref 13	ref 14	QM/MM
Ir−N(1)	2.169	2.177	2.205
Ir−N(1′)	2.130	2.146	2.146
Ir−H(1″)			1.577
Ir−H(2″)			1.573
N(1)−C(2)	1.369	1.362	1.364
N(1′)−C(2′)	1.374	1.359	1.361
C(2)−C(2′)	1.470	1.491	1.477
N(1)−Ir−N(1′)	76.6	76.6	75.5
P−Ir−P	161.8	167.3	165.6

[a] QM/MM refers to the geometry optimized within the ONIOM methodology. The numbering of the atoms is the same as in Chart 1.

The structure of the ion pair in solution as observed by NMR spectroscopy is thus the result of the preferred electrostatic interaction between the cation and the anion, as illustrated by the orientation of the dipole moment (Figure 5) and the topology of the electrostatic potential (Figure 6). The solid-state structure might then be a compromise between this preferred geometry for the ion pair and a more compact and more stable arrangement in the solid state. The liquid state being less constrained, the preferred electrostatic interaction is the leading contributor to the ion pair formation.

Conclusions

Two-dimensional homo- and heteronuclear NMR spectroscopies detect ion pairing for **1** and **2** in solution and identify the preferred structure of the ion pair. Instead of binding near the MH$_2$ group, which would give the closest M···anion distance and allow hydrogen bonding, the anion is located near the dipy ligand. The ion pairing is enhanced for smaller anions where the counteranion can approach closer to the cation. Since the solution and solid-state ion pair structures are different, crystallographic characterization has limited relevance to the

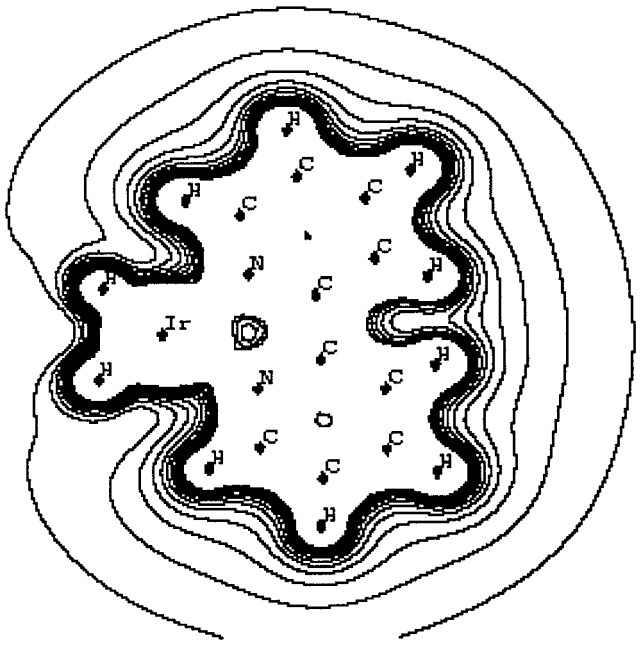

Figure 6. Contour plot of the electrostatic potential in the plane of the bipy ligand. Contour lines are from 0.08 to 0.3 au with a 0.02 increment between two consecutive contours.

solution case. Differences in ion pairing could affect structure and reactivity. This is of potential importance since reactions are usually carried out in solution in organic solvents, many of which favor ion pairing. Finally, we show how theory can satisfactorily explain the ion pair structure found in solution as a result of postive charge buildup at the ring junction (C-2 and C-2′) of the bipy ligand, not the N, as previously assumed; in contrast, all the atoms of the H_2IrN_2 fragment bear a negative charge.

Experimental Section

All operations were carried out under argon atmosphere using standard Schlenk techniques. Solvents were dried over calcium hydride (CH_2Cl_2) or sodium/benzophenone (Et_2O). Hexane was degassed prior use. IR spectra were recorded on a Midac M1200 FT-IR spectrometer. Microanalyses were carried out by Robertson Microlit Laboratories. One- and two-dimensional ^{1}H, ^{13}C, ^{19}F, and ^{31}P NMR spectra were measured on a Bruker DRX 400 NMR spectrometer. Referencing is relative to external TMS (^{1}H and ^{13}C), $CFCl_3$ (^{19}F), and 85% H_3PO_4 (^{31}P). NMR samples were prepared dissolving about 20 mg of compound in 0.6 mL of deuterated solvent. Two-dimensional ^{1}H NOESY and ^{19}F{^{1}H} HOESY spectra were recorded with a mixing time of 500−800 ms.

***cis,trans*-[IrH$_2$(bipy)(PRPh$_2$)$_2$]X (1, 2). Typical Procedure. For 2:** [Ir(cod)(PMePh$_2$)$_2$]PF$_6$ (1 equiv, 286.3 mg, 0.338 mmol) and 2,2′-bipyridyl (1 equiv, 53.0 mg, 0.338 mmol) were dissolved in degassed CH_2Cl_2 (10 mL). The resulting red solution was cooled to 0 °C. Dihydrogen gas was bubbled for 20 min, with constant stirring. To the orange solution, diethyl ether (100 mL) was added dropwise to precipitate 250.9 mg of beige solid (82.9%), which was obtained by filtration in vacuo, and dried in vacuo. Recrystallization is performed with CH_2Cl_2/Et_2O.

Characterization of *cis,trans*-[IrH$_2$(bipy)(PPh$_3$)$_2$]BF$_4$ (1a). ^{1}H NMR (CD_2Cl_2, 298 K): δ_H (ppm) 8.16 (ddd, $^3J_{2,3}$ = 5.5, $^4J_{2,4}$ = 1.6, $^5J_{2,5}$ = 0.8, 2), 8.00 (ddd, $^3J_{5,4}$ = 8.2, $^4J_{5,3}$ = 1.1, $^5J_{5,2}$ = 1.0, 5), 7.78 (ddd, $^3J_{4,3}$ = 7.6, $^3J_{4,5}$ = 8.2, $^4J_{4,2}$ = 1.6, 4), 7.38 (d, $^3J_{o,m}$ = 7.2, *o*), 7.35 (t, $^3J_{p,m}$ = 8.2, *p*), 7.28 (t, ($^3J_{m,p}$ + $^3J_{m,o}$)/2 = 7.5, *m*), 6.79 (ddd, $^3J_{3,4}$ = 7.6, $^3J_{3,2}$ = 5.5, $^4J_{3,5}$ = 1.3, 3), − 19.45 (t, $^2J_{H,P}$ = 16.6, H). ^{13}C{^{1}H} NMR (CD_2Cl_2, 298 K): δ_C (ppm) 156.0 (s, 6), 155.3 (s, 2), 137.5 (s, 4), 133.5 (t, $^2J_{o,P}$ = 6.1, *o*), 131.7 (t, $^1J_{ipso,P}$ = 27.0, *ipso*), 130.7 (s, *p*), 128.7 (t, $^3J_{m,P}$ = 5.0, *m*), 127.0 (s, 3), 123.8 (s, 5). ^{31}P{^{1}H} NMR (CD_2Cl_2, 298 K): δ_P (ppm) 21.4 (s, PPh_3). ^{19}F NMR (CD_2Cl_2, 298 K): δ_F (ppm) − 153.50 (br,$^{10}BF_4^-$), − 153.55 (q,$^1J_{F,B}$ = 1.0, $^{11}BF_4^-$). IR (thin film, cm^{-1}): ν(Ir−H) 2155.5, ν(BF_4) 1073.6. Anal. Calcd for $C_{46}H_{40}IrN_2P_2BF_4$·0.25CH_2Cl_2: C, 56.51; H, 4.15; N, 2.85. Found: C, 56.48; H, 4.13; N, 2.80. Yield: 83.6%.

Characterization of *cis,trans*-[IrH$_2$(bipy)(PPh$_3$)$_2$]PF$_6$ (1b). ^{1}H NMR (CD_2Cl_2, 298 K): δ_H (ppm) 8.17 (d, $^3J_{2,3}$ = 5.3, 2), 7.91 (d, $^3J_{5,4}$ = 8.2, 5), 7.76 (ddd, $^3J_{4,3}$ = 7.4, $^3J_{4,5}$ = 8.1, $^4J_{4,2}$ = 1.4, 4), 7.35 (m, *o* and *p*), 7.27 (t, ($^3J_{m,p}$ + $^3J_{m,o}$)/2 = 7.3, *m*), 6.80 (ddd, $^3J_{3,4}$ = 7.6, $^3J_{3,2}$ = 5.5, $^4J_{3,5}$ = 1.1, 3), − 19.44 (t, $^2J_{H,P}$ = 16.8, H). ^{13}C{^{1}H} NMR (CD_2Cl_2, 298 K): δ_C (ppm) 156.0 (s, 6), 155.4 (s, 2), 137.4 (s, 4), 133.5 (t, $^2J_{o,P}$ = 6.0, *o*), 131.7 (t, $^1J_{ipso,P}$ = 26.9, *ipso*), 130.7 (s, *p*), 128.7 (t, $^3J_{m,P}$ = 5.0, *m*), 127.1 (s, 3), 123.6 (s, 5). ^{31}P{^{1}H} NMR (CD_2Cl_2, 298 K): δ_P (ppm) 21.4 (s, PPh_3), − 143.16 (sept, $^1J_{P,F}$ = 711.0, PF_6^-). ^{19}F NMR (CD_2Cl_2, 298 K): δ_F (ppm) − 73.71 (d,$^1J_{F,P}$ = 711.0, PF_6^-). IR (thin film, cm^{-1}): ν(Ir−H) 2150.4, ν(PF_6) 836.9. Anal. Calcd for $C_{46}H_{40}IrN_2P_3F_6$·0.5CH_2Cl_2: C, 52.81; H, 3.91; N, 2.65. Found: C, 53.00; H, 3.78; N, 2.57. Yield: 84.1.

Characterization of *cis,trans*-[IrH$_2$(bipy)(PPh$_3$)$_2$]CF$_3$SO$_3$ (1c). ^{1}H NMR (CD_2Cl_2, 298 K): δ_H (ppm) 8.16 (d, $^3J_{2,3}$ = 5.4, 2), 8.04 (d, $^3J_{5,4}$ = 8.2, 5), 7.79 (ddd, $^3J_{4,3}$ = 7.6, $^3J_{4,5}$ = 8.2, $^4J_{4,2}$ = 1.5, 4), 7.38 (d, $^3J_{o,m}$ = 7.2, *o*), 7.35 (m, *o* and *p*), 6.79 (ddd, $^3J_{3,4}$ = 7.6, $^3J_{3,2}$ = 5.5, $^4J_{3,5}$ = 1.2, 3), −19.45 (t, $^2J_{H,P}$ = 16.8, H). ^{13}C{^{1}H} NMR (CD_2Cl_2, 298 K): δ_C (ppm) 156.1 (s, 6), 155.3 (s, 2), 137.5 (s, 4), 133.5 (t, $^2J_{o,P}$ = 6.1, *o*), 131.7 (t, $^1J_{ipso,P}$ = 27.0, *ipso*), 130.7 (s, *p*), 128.7 (t, $^3J_{m,P}$ = 4.9, *m*), 127.0 (s, 3), 123.9 (s, 5). ^{31}P{^{1}H} NMR (CD_2Cl_2, 298 K): δ_P (ppm) 21.4 (s, PPh_3). ^{19}F NMR (CD_2Cl_2, 298 K): δ_F (ppm) − 79.27 (s, $CF_3SO_3^-$). IR (thin film, cm^{-1}): ν(Ir−H) 2194.2. Anal. Calcd for $C_{46}H_{40}IrN_2P_2F_2SO_3$: C, 55.13; H, 3.94; N, 2.73. Found: C, 54.90; H, 3.84; N, 2.64. Yield: 82.2%.

Characterization of *cis,trans*-[IrH$_2$(bipy)(PPh$_3$)$_2$]BPh$_4$ (1d). ^{1}H NMR (CD_2Cl_2, 298 K): δ_H (ppm) 8.13 (d, $^3J_{2,3}$ = 5.3, 2), 7.55 (AB system, $^3J_{5,4}$ = 8.4, 4 and 5), 7.37 (m, *o*, o_X and *p*), 7.27 (m, *m*), 7.05 (t,$^3J_{m,o}$ = $^3J_{m,P}$ = 7.3, m_X), 6.90 (tt, $^3J_{p,m}$ = 7.2, $^4J_{p,o}$ = 1.2, p_X), 6.70 (m, 3), − 19.46 (t, $^2J_{H,P}$ = 16.8, H). ^{13}C{^{1}H} NMR (CD_2Cl_2, 298 K): δ_C (ppm) 164.5 (q, $^1J_{C,B}$ = 49.2, *ipso*$_X$), 155.7 (s, 6), 155.3 (s, 2), 137.3 (s, 4), 136.3 (s, o_X), 133.5 (t, $^2J_{o,P}$ = 6.1, *o*), 131.7 (t, $^1J_{ipso,P}$ = 26.9, *ipso*), 130.7 (s, *p*), 128.7 (t, $^3J_{m,P}$ = 5.0, *m*), 127.0 (s, 3), 126.0 (b, m_X), 123.4 (s, 5), 122.1 (s, p_X). ^{31}P{^{1}H} NMR (CD_2Cl_2, 298 K): δ_P (ppm) 21.4 (s, PPh_3). IR (thin film, cm^{-1}): ν(Ir−H) 2171.1. Anal. Calcd for $C_{70}H_{60}IrN_2P_2B$·1.5CH_2Cl_2: C, 64.98; H, 4.81; N, 2.12. Found: C, 65.26; H, 4.61; N, 1.85. Yield: 68.1%.

Characterization of *cis,trans*-[IrH$_2$(bipy)(PPh$_2$Me)$_2$]-PF$_6$ (2). ^{1}H NMR (CD_2Cl_2, 298 K): δ_H (ppm) 8.46 (dd, $^3J_{2,3}$ = 5.4, $^5J_{2,5}$ = 0.7, 2), 7.93 (d, $^3J_{5,4}$ = 8.0, 5), 7.87 (ddd, $^3J_{4,3}$ = 7.5, $^3J_{4,5}$ = 8.2, $^4J_{4,2}$ = 1.5, 4), 7.33 (m, *p*), 7.25 (m, *o* and *m*), 7.08 (ddd, $^3J_{3,4}$ = 7.1, $^3J_{3,2}$ = 5.5, $^4J_{3,5}$ = 1.4, 3), 1.88 (t Harris,[17b] |$^2J_{H,P}$ + $^4J_{H,P}$| = 6.4, PMePh$_2$), −19.87 (t, $^2J_{H,P}$ = 16.8, H). ^{13}C-{^{1}H} NMR (CD_2Cl_2, 298 K): δ_C (ppm) 155.9 (s, 6), 155.4 (s, 2), 137.5 (s, 4), 133.4 (t, $^1J_{ipso,P}$ = 26.7, *ipso*), 132.0 (t, $^2J_{o,P}$ = 6.0, *o*), 130.5 (s, *p*), 128.7 (t, $^3J_{m,P}$ = 5.0, *m*), 127.5 (s, 3), 123.8 (s, 5), 17.0 (t, |$^1J_{C,P}$ + $^3J_{C,P}$| = 37.6, PMePh$_2$). ^{31}P{^{1}H} NMR (CD_2Cl_2, 298 K): δ_P (ppm) − 0.27 (s, PMePh$_2$), − 143.14 (sept, $^1J_{P,F}$ = 711.0, PF_6^-). ^{19}F NMR (CD_2Cl_2, 298 K): δ_F (ppm) − 73.50 (d,$^1J_{F,P}$ = 711.0, PF_6^-). IR (thin film, cm^{-1}): ν(Ir−H) 2176.1, ν(PF_6) 836.2. Anal. Calcd for $C_{36}H_{36}IrN_2P_3F_6$: C, 44.62; H, 3.84; N, 2.74. Found: C, 44.58; H, 4.14; N, 2.75. Yield: 82.9%.

Structural Details. The structures of complexes **1b** and **1c** have been fully reported.[13,14] The nonbonded interionic distances were obtained from the crystal structures of **1b** and **1c**, registered in the Cambridge Structural Database System. The hydrogen atom positions of the bipyridyl ligand and the

hydride ligand positions were calculated. Use of TEXSAN software allowed the generation of the views of the solid-state structure of the complexes and counteranions.

Computational Details. All calculations were performed with the Gaussian 98 set of programs[18] with the ONIOM method.[19] The complex Ir(H)$_2$(bipy)(PPh$_3$)$_2^+$ was optimized at the ONIOM(B3PW91/UFF) level, where the QM part Ir(H)$_2$(bipy)(PH$_3$)$_2^+$ was optimized within the framework of density functional theory at the B3PW91 level.[20] The iridium atom was represented by the relativistic effective core potential (RECP) from the Stuttgart group (17 valence electrons) and its associated (8s7p5d)/[6s5p3d] basis set.[21] The phosphorus atoms were also treated with Stuttgart's RECPs and the associated basis set,[22] augmented by a polarization d function ($\alpha = 0.387$). A 6-31G(d,p) basis set was used for the hydrides and for both nitrogen atoms. The remaining atoms were treated by a 6-31G basis set. The molecular mechanics calculations were performed with the UFF force field.[23]

Natural population analysis (NPA)[24] and calculation of the electrostatic potential were performed on the QM part as obtained from the ONIOM calculation, namely, model complex Ir(H)$_2$(bipy)(PH$_3$)$_2^+$ with a frozen geometry as deduced from the ONIOM calculation. For these calculations Ir was treated as before and all the remaining atoms were described with the cc-pVDZ basis set of Dunning.[25]

Acknowledgment. This work was supported by grants from the Ministero dell'Università e della Ricerca Scientifica e Tecnologica (MURST, Rome, Italy), Programma di Rilevante Interesse Nazionale, Cofinanziamento 2000-1 (A.M., C.Z.), the CNRS and the University of Montpellier II (E.C.), and the NSF (R.H.C., K.G.).

OM010015L

(18) Frisch, M. J.; Trucks, G. W.; Schlegel, H. B.; Scuseria, G. E.; Robb, M. A.; Cheeseman, J. R.; Zakrzewski, V. G.; Montgomery, J. A.; Stratmann, R. E.; Burant, J. C.; Dapprich, S.; Millam, J. M.; Daniels, A. D.; Kudin, K. N.; Strain, M. C.; Farkas, O.; Tomasi, J.; Barone, V.; Cossi, M.; Cammi, R.; Mennucci, B.; Pomelli, C.; Adamo, C.; Clifford, S.; Ochterski, J.; Petersson, G. A.; Ayala, P. Y.; Cui, Q.; Morokuma, K.; Malick, D. K.; Rabuck, A. D.; Raghavachari, K.; Foresman, J. B.; Cioslowski, J.; Ortiz, J. V.; Stefanov, B. B.; Liu, G.; Liashenko, A.; Piskorz, P.; Komaromi, P. I.; Gomperts, G.; Martin, R. L.; Fox, D. J.; Keith, T.; Al-Laham, M. A.; Peng, C. Y.; Nanayakkara, A.; Gonzalez, C.; Challacombe, M.; Gill, P. M. W.; Johnson, B. G.; Chen, W.; Wong, M. W.; Andres, J. L.; Head-Gordon, M.; Replogle, E. S.; Pople J. A. *Gaussian 98*; Gaussian, Inc.: Pittsburgh, PA, 1998.

(19) Svensson, M.; Humbel, S.; Froese, R. D. J.; Matsubara, T.; Sieber, S.; Morokuma, K. *J. Phys. Chem.* **1996**, *100*, 19357.

(20) (a) Becke, A. D. *J. Chem. Phys.* **1993**, *98*, 5648. (b) Perdew, J. P.; Wang, Y. *Phys. Rev. B* **1992**, *82*, 284.

(21) Andrae, D.; Häussermann, U.; Dolg, M.; Stoll, H.; Preuss, H. *Theor. Chim. Acta* **1990**, *77*, 123.

(22) Bergner, A.; Dolg, M.; Küchle, W.; Stoll, H.; Preuss, H. *Mol. Phys.* **1990**, *30*, 1431.

(23) Rappe, A. K.; Casewitt, C. J.; Colwell, K. S.; Goddard, W. A.; Skiff, W. M. *J. Am. Chem. Soc.* **1992**, *114*, 10024.

(24) Reed, A. E.; Weinstock, R. B.; Weinhold, F. *J. Chem. Phys.* **1985**, *83*, 735.

(25) Dunning, T. H., Jr. *J. Chem. Phys.* **1989**, *90*, 1007.